Macromolecular Rapid Communications
www.mrc-journal.de

The Topology of Polymer Brushes Determines Their Nanoscale Hydration

Apostolos Vagias, Andrew Nelson, Peixi Wang, Julija Reitenbach, Christina Geiger, Lucas Philipp Kreuzer, Thomas Saerbeck, Robert Cubitt, Edmondo Maria Benetti,* and Peter Müller-Buschbaum*

Time-of-flight neutron reflectometry (ToF-NR) performed under different relative humidity conditions demonstrates that polymer brushes constituted by hydrophilic, cyclic macromolecules exhibit a more compact conformation with lower roughness as compared to linear brush analogues, due to the absence of dangling chain ends extending at the polymer–vapor interface. In addition, cyclic brushes feature a larger swelling ratio and an increased solvent uptake with respect to their linear counterparts as a consequence of the increased interchain steric repulsions. It is proposed that differences in swelling ratios between linear and cyclic brushes come from differences in osmotic pressure experienced by each brush topology. These differences stem from entropic constraints. The findings suggest that to correlate the equilibrium swelling ratios at different relative humidity for different topologies a new form of the Flory-like expression for equilibrium thicknesses of grafted brushes is needed.

1. Introduction

Polymer topology effects by cyclic macromolecules have been investigated for decades, especially focusing on how a shift in polymer topology from linear to cyclic influences the properties of bulk polymers, melts, and solutions.[1–14] The absence of chain ends in cyclic polymers markedly influences their structural and dynamic characteristics within crowded environments.[15–17] For instance, the diffusion coefficient of cyclic macromolecules in melts was found to be twice as large compared to that of linear chains with the same molar mass and composition. In addition, the squared ratio of gyration radius (R_g) between linear and cyclic polymers in solutions under theta solvent conditions was predicted to be about two, with (R_g) showing a Flory scaling exponent (ν) of 0.4, in between the values for Gaussian conformation ($\nu = 0.5$) and poor solvent ($\nu = 0.3$) state.[15,18,19]

Within solutions, ring polymers feature enhanced effective interchain repulsions due to stronger excluded volume interactions with respect to their linear counterparts of comparable molar mass, whereas polymer segment–solvent interactions are more favored.[8,20–23] In addition, the cloud points in aqueous solutions for amphiphilic, cyclic polymers are significantly higher compared to those recorded for their linear homologues. Hence, although cyclic macromolecules are intrinsically more compact, they are also expected to solvate more favorably when compared to compositionally identical linear polymers.[20,24]

A. Vagias, L. P. Kreuzer, P. Müller-Buschbaum
Heinz Maier-Leibnitz Zentrum (MLZ)
Technical University of Munich
Lichtenbergstr. 1, 85748 Garching, Germany
E-mail: apostolos.vagias@frm2.tum.de

A. Nelson
ANSTO
New Illawarra Road, Lucas Heights, NSW 2234, Australia

The ORCID identification number(s) for the author(s) of this article can be found under https://doi.org/10.1002/marc.202300035

DOI: 10.1002/marc.202300035

P. Wang, J. Reitenbach, C. Geiger, L. P. Kreuzer, P. Müller-Buschbaum
Technical University of Munich
TUM School of Natural Sciences
Department of Physics
Chair for Functional Materials
James-Franck-Str. 1, 85748 Garching, Germany

T. Saerbeck, R. Cubitt
Institut Laue Langevin (ILL)
71 Avenue des Martyrs, Grenoble 38000, France

E. M. Benetti
Polymer Surfaces Group
Department of Chemical Sciences
University of Padova
Via Marzolo 1, Padova 35122, Italy
E-mail: edmondo.benetti@unipd.it

E. M. Benetti
Laboratory for Surface Science and Technology
Department of Materials
ETH Zürich
Vladimir-Prelog-Weg 5, Zürich 8093, Switzerland

Interestingly, the presence of a confining substrate can amplify these and other topology effects.[25–30] Due to their reduced molecular dimensions, cyclic polymers can generate significantly denser polymer brushes when grafted on macroscopic surfaces and nanoparticles (NPs). Especially on NPs, this phenomenon provides increased colloidal stability and augmented hindrance toward unspecific interaction with serum proteins.[24,31]

Alternatively, cyclic polymer brushes on macroscopic surfaces showed extreme lubricity when sheared against identical brush counter surfaces, due to the absence of dangling chain ends that typically favor interpenetration between the opposing linear brush layers.[32]

These initial results demonstrated that, for a given polymer composition and molar mass, several technologically relevant interfacial properties of polymer brushes can be strongly altered by changing chain topology. However, topology-dependent interactions with the surrounding medium have been barely explored; in particularly, the influence of grafted chain-topology on solvent–polymer brush interactions. Varying brush hydration determines an array of different interfacial properties, including lubrication,[33,34] steric stabilization of the surface,[35] and resistance toward unspecific protein adsorption.[36,37] It has so far not been explored how differences in brush topology, from linear to cyclic, may manifest in swelling and how interactions may reflect on swelling. In particular, since many sensor platforms operate with brushes that can harvest vapor or sense humidity alterations, [38–41] the elucidation of water vapor distribution in brushes can be insightful.

In this work, we exploit time-of-flight neutron reflectometry (ToF-NR) to investigate the hydration behavior of linear and cyclic poly(2-ethyl-2-oxazoline) brushes (L-PEOXA and C-PEOXA, respectively) for three swelling/drying cycles when subjected to water vapor exposure, especially focusing on how the chain topology determines the tendency of polymer brushes to associate water molecules. Neutrons enable achieving a high scattering contrast when deuterated water (D_2O) is adsorbed by a protonated polymer brush grafted on a macroscopic surface.[42,43] Through ToF-NR, the brush thickness response to a variation of relative humidity (RH) is evaluated with precise spatiotemporal resolution.[44] The additional and unique advantage of ToF-NR is that the scattering length density (SLD) profile normal to the substrate can be obtained and used to resolve the distribution of polymer and solvent density across the sample plane independently from brush thickness. In a subsequent work, we will address the effects of kinetics in those topologies.

2. L-PEOXA and C-PEOXA Brush Assemblies

L-PEOXA and C-PEOXA brushes were grafted on TiO_2 substrates through an assembly of poly-L-lysine-*g*-PEOXA (PLL-*g*-PEOXA) copolymers,[32] which included a positively charged PLL backbone ($M_n \approx 20$ kDa) and PEOXA side chains presenting either linear (number-averaged molecular weight $M_n = 11.5$ kDa, polydispersity index $Đ = 1.1$) or cyclic topology ($M_n = 9.2$ kDa, $Đ = 1.2$). According to the brush structure obtained through graft copolymer adsorption,[45] PLL segments interact preferentially with the negatively charged TiO_2 substrate, while PEOXA chains stretch out away from the substrate. Radii of gyration for L-PEOXA ($R_{g,L} \approx 5.34$ nm) and C-PEOXA ($R_{g,C} \approx 3.78$ nm) have been calculated by the experimentally determined weight-averaged molecular weights (M_w)[32] and the intrinsic viscosity.

Table 1. Values of grafting density (σ), dimensionless degree of grafted chain overlap ($\zeta = \Upsilon/2R_g$) and reduced dimensionless grafting density (Σ) for C-PEOXA and L-PEOXA.

Topology	σ [chains nm^{-2}]	$\zeta = \Upsilon/2R_g$	Σ
C-PEOXA	0.25	0.28	0.10
L-PEOXA	0.3	0.18	0.12

The dimensional grafting density (σ) corresponded to $\sigma_L = 0.30$ and $\sigma_C = 0.25$ chains nm^{-2} for L-PEOXA and C-PEOXA respectively. The distance (Υ) between grafted PEOXA chains was calculated, as $\Upsilon_L \approx 1.95$ nm and $\Upsilon_C \approx 2.15$ nm, by using $\Upsilon = (\frac{2}{\sqrt{3}\sigma})^{1/2}$. As last, the dimensionless ratio $\zeta = \Upsilon/2R_g$ was calculated as 0.18 (L-PEOXA) and 0.28 (C-PEOXA), using the respective values ($R_{g,L}$, Υ_L) or ($R_{g,C}$, Υ_C).[32] The values of reduced dimensionless grafting density ($\Sigma = \sigma b^2$), using $b = 0.63$ nm as an effective monomer size[46] ($\Sigma = \sigma b^2$), were $\Sigma = 0.10$ and $\Sigma = 0.12$, for cyclic and linear brushes, respectively. These parameters are shown in **Table 1**.

The degree of polymerization for both L-PEOXA and C-PEOXA[32] ($N \approx 100$) is smaller than the cut-off N_o, where knots could form for C-PEOXA ($N < N_o \approx 300$),[47] hence the C-PEOXA rings are unknotted. The surface overlap concentration[29] of the grafted brushes σ^*, was determined to be $\sigma^*_L = 6 \times 10^{-3}$ and $\sigma^*_C = 1.2 \times 10^{-2}$ chains nm^{-2}. Since $\sigma > \sigma^*$ for both topologies, the surface-grafted polymers adopt a brush-like conformation where interchain interactions are present.

3. Swelling of L-PEOXA and C-PEOXA Brushes

L- and C-PEOXA brushes were subsequently analyzed by ToF-NR after subjected to different relative humidity (RH) values.[48,49] Interaction with water vapor and conformation of L- and C-PEOXA brushes were specifically investigated under "dry" and "swollen" conditions, which corresponded to $RH = 3\%$ and $RH = 95\%$, respectively (**Scheme 1**).

ToF-NR measurements were performed at the D17 reflectometer[44] at the Institute Laue Langevin (ILL), which is equipped with a polychromatic divergent beam in the out-of-reflection-plane that ensures maximum neutron flux for performing measurements while varying RH.[50] A broad wavelength (λ) band of $\lambda = 2$–27 Å with a spectral resolution ($\Delta\lambda/\lambda$) of 10% was applied during the measurements. Static ToF-NR experiments were carried out at two incident angles (α_i) of $\alpha_i = 0.5°$ and $\alpha_i = 2.5°$, allowing to cover a broad q_z-range and thus to probe with finer detail the SLD profiles and thicknesses in the dry and fully swollen states. Here, q_z denotes the momentum transfer vertical to the sample surface.

Following a coherent summation method for data reduction,[51] reflectivity (R) curves for a q_z-range between $q_z = 0$ Å^{-1} and $q_z = 0.23$ Å^{-1} are reported in **Figure 1**a,b, for C-PEOXA and L-PEOXA, respectively. Using refnx software for model-fitting,[52] the best fits to the ToF-NR curves for both brush types were obtained by applying a slab-multilayer model that sequentially included silicon (Si) (backing layer), a single

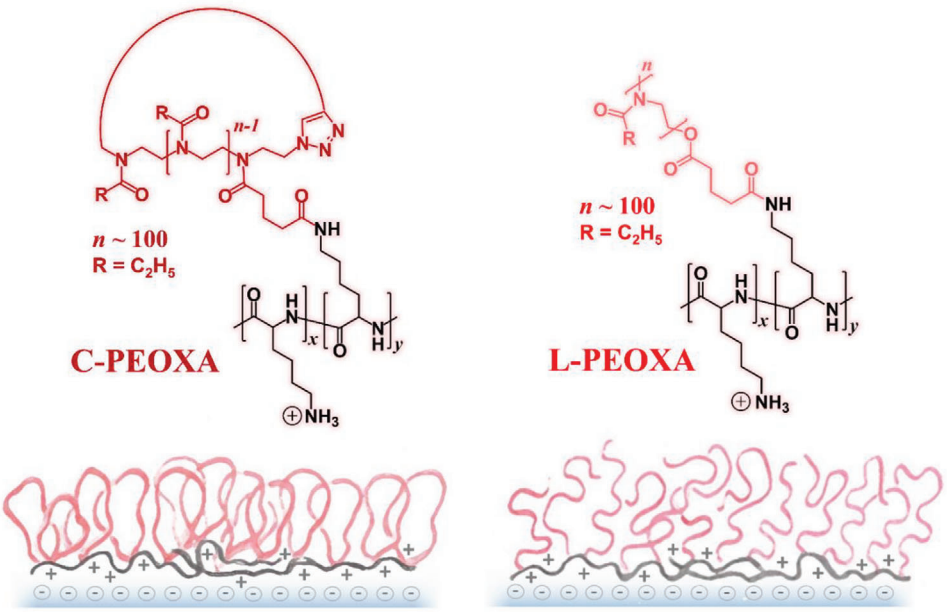

Scheme 1. Schematic representation and chemical composition of C-PEOXA and L-PEOXA brushes obtained from the assembly of the corresponding graft copolymers on TiO_2 substrates.

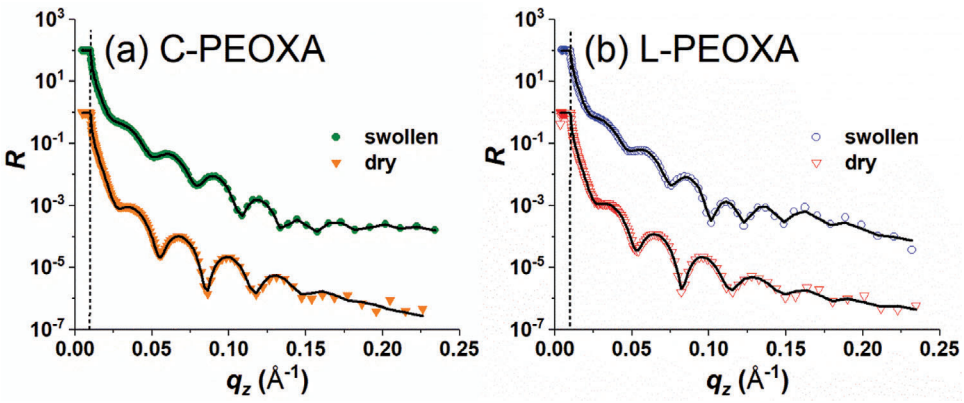

Figure 1. Static ToF-NR curves recorded on a) C-PEOXA brushes at high (= 95%) and low (= 3%) values of *RH* (circles and triangles, respectively) and b) L-PEOXA brushes at high and low *RH* (circles and triangles, respectively). The error bars for the reflectivity are within the size of the experimental dataset symbol. The black lines are the model fits. Vertical dashed black lines correspond to the critical edge of the brushes. The reflectivity curves have been multiplied by an arbitrary vertical shifting factor for clarity.

amorphous silicon oxide (SiO_x) layer, a single TiO_2 layer and different numbers of PLL-*g*-PEOXA layers. This description of polymer brushes swollen by water vapor agreed well with the modeling recently proposed by van Eck et al. for vapor-swollen brushes.[53] A detailed summary of calculations can be found in **Tables** S1–S4 and **Figure** S1 (Supporting Information, including alternative model-fits[54]). An increase in the frequency of the Kiessig fringes could be clearly recorded while switching from the dry to the swollen state.

The model SLD profiles for linear and cyclic brushes under "dry" and "swollen" states (low and high values of *RH*) are shown in **Figure 2**a,b for C- and L-PEOXA, respectively.

Interestingly, at relatively low *RH* (= 3%) values, a slight but non-negligible increase in SLD for z values between the TiO_2 layer (region 3, at z = 0 Å) and the polymer brush layer (region 4, at z = 12 Å) suggests an apparent D_2O enrichment at the substrate/brush interface. The fits were not possible without the presence of this weak upturn in SLD. The apparently large values of SLD next to the TiO_2 layer ($SLD_{dry,\ region\ 4} \approx 2.5$ ($\times 10^{-6}$ Å^{-2})> $SLD_{dry,PEOXA}$ = 0.985 ($\times 10^{-6}$ Å^{-2})) in the dry state (*RH* = 3%) might imply the fast adsorption of D_2O molecules probably from ambient atmosphere -even before exposure to D_2O vapor- near the grafting surface, which presumably took place at much shorter timescales compared to the time required for acquiring the individual datasets. Alternatively, this phenomenon might be due to the strong interaction between D_2O and partially charged PLL backbones, which preferentially interact with (and lay down on) the TiO_2 surface and were more hygroscopic than the PEOXA

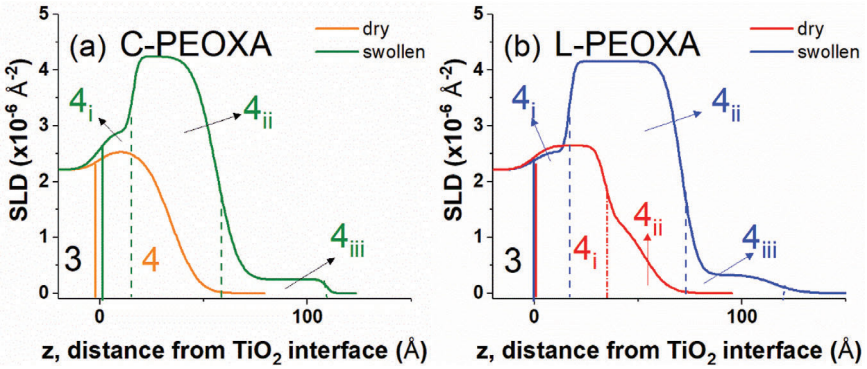

Figure 2. SLD profiles along the sample's normal direction (z) for a) C-PEOXA and b) L-PEOXA brushes under dry and swollen states obtained by model-fitting ToF-NR curves. Along each SLD profile, the different layers constituting the samples are identified as: Si (region 1), SiO_x (region 2), TiO_2 layer (region 3) and the different polymeric slab layers at $z > 0$ Å (region 4). Vertical dashed and dashed-dotted lines highlight the boundaries between the different polymeric slab layers (4_i, 4_{ii}...). Vertical solid (colored) lines refer to the substrate–brush interface. The profiles are aligned ($z = 0$) at the TiO_2 substrate to show the changes in SLD occurring in the polymer film.

grafts.[55] It is also known that the amide groups can be subject to H/D exchange, as reported for PNIPAM-based films and microgels.[49,56] FTIR studies on amide-containing thin polymer films suggest that H/D exchange on amide bonds can take place over few minutes.[57] Such effects become substantial due to the small thickness of the examined brush layers. Considering the small brush thickness, it is not unlikely that residual D_2O molecules from the surrounding atmosphere next to the sample diffuse and contribute to the H/D exchange at timescales much faster than a full swelling/drying cycle (≈2 h acquisition by ToF-NR) of these brushes.

The comparison of the overall thicknesses derived from the SLD profiles reported in **Figure 2** (also **Figure** S1 for full SLD profiles with substrate contribution, Supporting Information) (especially considering swollen regions (4_{ii}) and (4_{iii})) suggests that C-PEOXA brushes adopt a more compact conformation with respect to L-PEOXA analogues, both in dry and swollen states. One could alternatively extract the density profiles from the SLD profiles,[58] considering that the SLD profiles can also be described as linear combination of nominal SLD values and that mass conservation requires that the sum of the volume fractions ($\sum_{i=1}^{N} \phi_i$) in the polymer region is equal to 1 ($\sum_{i=1}^{N} \phi_i = 1$):

$$\mathrm{SLD}(z) = (\mathrm{SLD}_{\mathrm{dry,PEOXA}}) \cdot \Phi_{\mathrm{PEOXA}}(z) + (\mathrm{SLD}_{\mathrm{D2O}}) \cdot \Phi_{\mathrm{D2O}}(z) \quad (2a)$$

$$\Phi_{\mathrm{PEOXA}}(z) + \Phi_{\mathrm{D2O}}(z) + \Phi_{air}(z) = 1 \quad (2b)$$

Due to the challenge into an in-depth interpretation of the SLD profiles in the dry state for either sample, it is nontrivial to decouple the contributions of air, PEOXA and D_2O. Hence, we refrain from making further assumptions and present SLD profiles everywhere in the manuscript. Since more complex models using parabolic density profiles are ruled out (Supporting Information), the density profiles for L-PEOXA and C-PEOXA could very likely be described by a step function. Interestingly, the SLD profile of L-PEOXA brushes in the region (4_{iii}) decays more gradually with increasing z, i.e., moving from the grafting surface toward the air–brush interface, when compared to the C-PEOXA brush. This suggests a larger roughness at the polymer–air interface for L-PEOXA. These findings agree well with previously reported computational studies,[27,29] which suggested that cyclic brushes exhibit a more uniform and compact monomer density profile, which is characterized by a sharper brush interface with respect to their linear counterparts. Based on the differences in the SLD profiles at the polymer–air interface reported in **Figure 2**, we propose a non-uniform distribution of dangling chain ends to be present on L-PEOXA brushes along z, whereas for C-PEOXA analogues the sharper decay of the SLD profile points to a uniform monomer distribution.

Morgese et al. previously reported that the presence of chain ends for L-PEOXA and their uneven distribution across the brush thickness favors interpenetration between two L-PEOXA coated counter-surfaces slid against each other under relatively high normal pressures, a phenomenon that typically leads to an increase in friction between linear brush surfaces.[59] In contrast, interpenetration is not favored between opposing cyclic-brush surfaces,[60] leading to efficient hampering of dissipative forces and a much higher lubricity.[32]

Swelling experiments were repeated three times, subjecting L- and C-PEOXA brushes to a progressive increase in RH from 3% to 95%, each of them followed by a decrease of RH from 95% to 3%. Based on the ToF-NR results, we also examine the reproducibility in water vapor uptake and release for both systems, in terms of swelling ratios (SR), expressed as thickness ratios ($SR = h_{\mathrm{swollen}}/h_{\mathrm{dry}}$), ratio ($A'$) of areas ($A$) under the SLD profile ($A' = \frac{A_{\mathrm{swollen}}}{A_{\mathrm{dry}}}$) and root mean square roughness (R_q). The thickness (h_{swollen}, or, h_{dry}) was determined as a sum of thicknesses from the individual layers used in model fits. As reported in **Table 2**, C-PEOXA exhibited significantly higher SR and A' values compared to L-PEOXA ($SR_{\mathrm{C,\,static}} > SR_{\mathrm{L,\,static}}$; $A'_{\mathrm{C,\,static}} > A'_{\mathrm{L,\,static}}$). The same holds for the volumetric amount of D_2O ($Q'_{\mathrm{C,\,static}} > Q'_{\mathrm{L,\,static}}$), the values of which have been calculated as:

$$Q' = Q'_{\mathrm{swollen}} - Q'_{\mathrm{dry}} = \left[\frac{\mathrm{SLD}_{\mathrm{measured,swollen}} - \mathrm{SLD}_{\mathrm{dry,PEOXA}}}{\mathrm{SLD}_{\mathrm{D2O}} - \mathrm{SLD}_{\mathrm{dry,PEOXA}}}\right] - \left[\frac{\mathrm{SLD}_{\mathrm{measured,dry}} - \mathrm{SLD}_{\mathrm{dry,PEOXA}}}{\mathrm{SLD}_{\mathrm{D2O}} - \mathrm{SLD}_{\mathrm{dry,PEOXA}}}\right] \quad (3)$$

Table 2. Swelling ratios (SR), volumetric amount of solvent (Q'), areas under the SLD profile (A') and root mean squared roughness (R_q) at the polymer–air interface from the modeling of static ToF-NR curves in the swollen state for each topology and for each cycle number.

Cycle number	SR_L	SR_C	Q'_L [vol%]	Q'_C [vol%]	A'_L	A'_C	$R_{q,L}$ [nm]	$R_{q,C}$ [nm]
1	2.2	3.2	28	33	2.4	2.6	9.7 ± 2.2	2.9 ± 6.8
2	1.7	3.3	26	29	2.3	2.6	10.0 ± 1.1	2.6 ± 4.1
3	1.6	3.5	25	27	2.2	2.6	9.9 ± 0.9	4.4 ± 1.9

We obtained $Q'_{C-PEOXA} = 0.29 \pm 0.03$, while $Q'_{L-PEOXA} = 0.26 \pm 0.01$. For the calculation of Q', the $SLD_{measured}$ in the layer with the largest SLD (layer 4_{ii}) was used. Both A' and $Q'$are reported, as being similar quantities and both proportional to the amount of water uptake. We note again that the C-PEOXA presents unknotted and non-concatenated cyclic brushes.

Under these conditions, the topological constraints take some form of entropic penalties between monomers in the free energy expression of polymer conformation. Such constraints have been reported for free energy expressions of concentrated solutions of cyclic polymers.[61,62] When proximity to a planar substrate comes into play, dissipative particle dynamics (DPD) simulations performed by Jehser and co-workers predicted a larger solvent uptake on cyclic brushes than for linear brushes of comparable molar mass, due to the steric constraints intrinsic to the cyclic topology, manifested by stronger excluded volume interactions.[29] The increased water association by cyclic brushes agreed well with molecular dynamics simulations previously reported by Hossain et al. in the case of cyclic polystyrene (PS) in a good solvent, where the expansion factor for cyclic PS was found to be significantly larger than that characteristic of its linear analogue. This was due to stronger excluded volume interactions, which lead to stronger repulsions between monomer segments within cyclic polymers compared to those characteristics of their linear counterparts.[22]

We expect that enhanced interchain steric repulsions exist between C-PEOXA brushes along the sample surface. These repulsions facilitate water uptake as a way to bypass the lateral constraints. This interpretation also agrees with the recent simulations by Wan and co-workers, where smaller stretching energies were calculated for cyclic brushes than linear ones, due to increase in excluded volume interactions because of the topology constraints in cyclic ones.[27]

The more compact character of the conformation of C-PEOXA brushes upon hydration also influences their surface roughness. By comparing the decay in the SLD profiles (especially the regions of 4_{iii} in Figure 2) at the polymer–air interface and the values of R_q for L- and C-PEOXA brushes ($R_{q,L} > 2 \cdot R_{q,c}$) (Table 2), the hydrated polymer–air surface of C-PEOXA brushes appears significantly smoother compared to that of L-PEOXA.

These experimental observations can be rationalized with thermodynamic arguments. We use a mean-field Flory-like expression from regular solution theory for thin films to compare the topology-dependent differences in swelling. De Beer and co-workers[53] proposed a modified version of the regular solution theory for thin polymer brush layers exposed to vapor. Following Galvin and co-workers,[63] we define a solvent effective volume fraction $\varphi_{s,D2O}$ as the ratio $\varphi_{s,D2O} = \frac{h_{swollen} - h_{dry}}{h_{swollen}}$ from the measured total thicknesses in the swollen ($h_{swollen}$) and dry (h_{dry}) state. The quantity $\varphi_{s,D2O}$ is bound between 0 and 1. The free energy expression considers as input parameters the RH, the $\varphi_{s,D2O}$ and—in addition to previous expressions used for chains in the form of physically cross-linked polymer network—the dimensionless parameter Σ. The chemical potential of the solvent inside the brush matches the one in the solvent vapor surrounding the brush. The chemical potential outside the brush relates to the partial vapor pressure.[64] On the basis of the regular solution theory and by considering that the chains are grafted, we can write :

$$\ln\left(\frac{P}{P_{sat}}\right) = \left(1 - \varphi_{s,D2O}\right) + \ln(\varphi_{s,D2O}) + \chi_{eff} \cdot \left(1 - \varphi_{s,D2O}\right)^2 + \frac{3 \cdot \Sigma^2}{\left(1 - \varphi_{s,D2O}\right)} \quad (4)$$

Considering that $\frac{P}{P_{sat}} = RH = 95\%$ and by inserting the particular values for $\varphi_{s,D2O}$ ($\varphi_{s,D2O,\,L1} = 0.54$; $\varphi_{s,D2O,\,C1} = 0.68$) and Σ (Table 1) in Equation (4), we obtain $\chi_{eff,C1} \approx 0.82$, while $\chi_{eff,L1} \approx -0.02$. However, this calculation disagrees with our ToF-NR results presented in Table 2, where the two topologies are found to reach different SR (and hence $\varphi_{s,D2O}$). Hence, this apparent outcome ($\chi_{eff,C1} > \chi_{eff,L1}$) cannot explain the larger solvent uptake for C-PEOXA. Additional contributions, as, e.g., from topological constraints for the case of C-PEOXA grafted brushes must be taken into account. Cates and Deutsch[16] and later Sakaue[61,62,65] presented two entropic terms in the free energy expression for polymer rings in dense solutions. One term to account for the non-concatenation between rings and another one for squeezing the ring while maintaining a constant unknotting constraint. It is for the moment unclear whether the enhanced solvent vapor uptake for C-PEOXA stems exclusively from enhanced excluded volume interactions, but this seems to be at least one possible reason behind the swelling differences.

Starting from an entanglement molecular weight ($M_e = 1800$ g mol^{-1}) for the melt state ($\varphi_{s,D2O} = 0$; $\varphi_{PEOXA} = 1$) of L-PEOXA, under the assumption that this is similar to the one of linear PEO,[66] we calculated the effective entanglement molecular weight ($M_{e,eff}$) in our swollen brushes, at their respective φ_{PEOXA} ($= 1 - \varphi_{s,D2O}$):

$$M_{e,eff} = \frac{M_e}{\varphi_{PEOXA}} \quad (5)$$

We obtained $M_{e,eff,\,L-PEOXA} = 4000$ g mol^{-1} and $M_{e,eff,\,C-PEOXA} = 5800$ g mol^{-1}, from which the effective number of entanglements ($N_{e,eff} = \frac{M_w}{M_{e,eff}}$) was calculated: $N_{e,eff,\,L-PEOXA} = 2.88$ and $N_{e,eff,\,C-PEOXA} = 1.59$. The osmotic pressure contribution (Π_{osm}) in dense polymer solutions can be described as:[65]

$$\Pi_{osm} \approx \frac{\varphi^3_{PEOXA}}{N_{e,eff}} \quad (6)$$

We assume that this expression also holds in our dense grafted brush systems. We then calculate $\Pi_{osm,L-PEOXA}$(= 0.0316) > $\Pi_{osm,C-PEOXA}$ (= 0.0187). This outcome would suggest larger SR values for L-PEOXA and would thus contradict

our experimental findings (Table 2). The larger water uptake by C-PEOXA is a robust experimental finding. Hence, $\Pi_{osm,C-PEOXA} \geq \Pi_{osm,L-PEOXA}$. For cyclic brushes, it is not trivial to identify the exact length of topological constraints, in contrast to dense linear polymer networks in bulk. However, we can estimate an upper value for the cut-off size for the topological length over which constraints are set in for C-PEOXA. If we assume (in)equality in osmotic pressure contributions ($\Pi_{osm,C-PEOXA} \geq \Pi_{osm,L-PEOXA}$) and use as input values the experimentally obtained φ_{PEOXA}, we can back-calculate a minimum value for a new effective number of entanglements, $N'_{e,eff,C-PEOXA} \approx 0.94$. Using a Kuhn length ($l_k$) of $l_{k,PEOXA} = 1.4$ nm, we obtain a maximum cut-off size for the average distance ($\alpha_{max} = 1.35$ nm) between topological constraints for C-PEOXA, following the equation for the tube diameter by Doi and Edwards:[67]

$$\alpha_{max} = lk, \text{PEOXA} \cdot N\prime^{1/2}_{e,eff,C-PEOXA} \quad (7)$$

Note that $\alpha_{max} < \Upsilon_C$ (≈ 2.15 nm). Hence, our analysis suggests that Υ_C is most likely an overestimated input for a reasonable N_e calculation in the case of swelling for cyclic brushes. This suggests that the actual grafting density is a necessary but not adequate condition for describing the mismatch in water vapor uptake between the two topologies. Since $\sigma > \sigma^*$ holds for these brushes and by comparing to simulations from Jehser et al.,[29] it is not unlikely that an anisotropic expansion of the cyclic polymer brush takes place with much more enhanced swelling across the brush thickness rather than along the substrate. Due to the increased repulsive interchain interactions, we also believe that the cyclic geometry offers less spatial restrictions for solvent molecules to fill the free space between polymer regions and hence renders solvation less challenging.

4. Conclusions

Correlations between topology of brushes and solvent vapor uptake—so far elusive—are experimentally explored for the first time. Our study reveals coupling between geometrical characteristics of the brush nanostructure and solvent distribution in brush-forming graft copolymer with linear versus cyclic side chains. The data obtained from ToF-NR suggest a more compact conformation, higher water uptake and smoother polymer–vapor interface for cyclic PEOXA brushes, when compared to their linear counterparts of comparable molar mass. The existing Flory–Huggins expressions for grafted brushes break down in the case of cyclic brush conformation. Hence, alternative reasons, including contributions from topological constraints for the cyclic conformation, are needed to rationalize differences in solvent vapor uptake. A new free energy expression would enable an independent theoretical support for the differences manifested in the ToF-NR experimental findings. We hope that our results will drive additional explorations by combined simulations and experiments.

Supporting Information

Supporting Information is available from the Wiley Online Library or from the author.

Acknowledgements

The authors acknowledge funding from the German Ministry for Education and Research (BMBF) withi'n the project "FlexiProb" (Grant No. 05K2016). The authors would like to thank Stéphanie Jimenez for her precious technical support during the experiments at the neutron reflectometer D17. The Institut Laue-Langevin and the neutron reflectometer D17 are acknowledged for beam time allocation and excellent equipment and support of measurements. P.W. acknowledges the China Scholarship Council (CSC). A.V. would like to thank Oleg Borisov for helpful discussions.

Open access funding enabled and organized by Projekt DEAL.

Conflict of Interest

The authors declare no conflict of interest.

Data Availability Statement

The data that support the findings of this study are available from the corresponding author upon reasonable request.

Keywords

cyclic polymers, grafted brushes, neutron reflectometry, swelling

Received: January 23, 2023
Published online: March 13, 2023

[1] A. Rosa, R. Everaers, *PLoS Comput. Biol.* **2008**, *4*, e1000153.
[2] F. M. Haque, S. M. Grayson, *Nat. Chem.* **2020**, *12*, 433.
[3] Y. Kobayashi, Y. Doi, S. S. Abdul Rahman, E. Kim, T.-H. Kim, A. Takano, Y. Matsushita, *Macromolecules* **2018**, *51*, 1885.
[4] G. B. Mckenna, G. Hadziioannou, P. Lutz, G. Hild, C. Strazielle, C. Straupe, P. Rempp, A. J. Kovacs, *Macromolecules* **1987**, *20*, 498.
[5] B. Li, Z. Sun, L. An, Z.-G. Wang, *Sci. China: Chem.* **2016**, *59*, 619.
[6] T. E. Gartner, F. M. Haque, A. M. Gomi, S. M. Grayson, M. J. A. Hore, A. Jayaraman, *Macromolecules* **2019**, *52*, 4579.
[7] S. Y. Reigh, D. Y. Yoon, *ACS Macro Lett.* **2013**, *2*, 296.
[8] T. Iwamoto, Y. Doi, K. Kinoshita, A. Takano, Y. Takahashi, E. Kim, T.-H. Kim, S.-I. Takata, M. Nagao, Y. Matsushita, *Macromolecules* **2018**, *51*, 6836.
[9] D. G. Tsalikis, T. Koukoulas, V. G. Mavrantzas, R. Pasquino, D. Vlassopoulos, W. Pyckhout-Hintzen, A. Wischnewski, M. Monkenbusch, D. Richter, *Macromolecules* **2017**, *50*, 2565.
[10] M. Kapnistos, M. Lang, D. Vlassopoulos, W. Pyckhout-Hintzen, D. Richter, D. Cho, T. Chang, M. Rubinstein, *Nat. Mater.* **2008**, *7*, 997.
[11] S. Gooßen, A. R. Brás, M. Krutyeva, M. Sharp, P. Falus, A. Feoktystov, U. Gasser, W. Pyckhout-Hintzen, A. Wischnewski, D. Richter, *Phys. Rev. Lett.* **2014**, *113*, 168302.
[12] D. Magerl, M. Philipp, E. Metwalli, P. Gutfreund, X.-P. Qiu, F. M. Winnik, P. Müller-Buschbaum, *ACS Macro Lett.* **2015**, *4*, 1362.
[13] L. Zhang, R. Elupula, S. M. Grayson, J. M. Torkelson, *Macromolecules* **2016**, *49*, 257.
[14] N. Jiang, J. Chen, T. Yu, A. Chao, L. Kang, Y. Wu, K. Niu, R. Li, M. Fukuto, D. Zhang, *Macromolecules* **2020**, *53*, 7601.
[15] B. H. Zimm, W. H. Stockmayer, *J. Chem. Phys.* **1949**, *17*, 1301.
[16] M. E. Cates, J. M. Deutsch, *J. Phys. (Paris)* **1986**, *47*, 2121.
[17] M. Müller, J. P. Wittmer, M. E. Cates, *Phys Rev E* **1996**, *53*, 5063.
[18] E. F. Casassa, *J. Polym. Sci., Part A: Gen. Pap.* **1965**, *3*, 605.
[19] J. Roovers, *J. Polym. Sci., Polym. Phys. Ed.* **1985**, *23*, 1117.

[20] X.-P. Qiu, F. Tanaka, F. M. Winnik, *Macromolecules* **2007**, *40*, 7069.
[21] A. Takano, Y. Ohta, K. Masuoka, K. Matsubara, T. Nakano, A. Hieno, M. Itakura, K. Takahashi, S. Kinugasa, D. Kawaguchi, Y. Takahashi, Y. Matsushita, *Macromolecules* **2012**, *45*, 369.
[22] M.d. D. Hossain, J. C. Reid, D. Lu, Z. Jia, D. J. Searles, M. J. Monteiro, *Biomacromolecules* **2018**, *19*, 616.
[23] J. Zhou, J. Yang, M. W. Ishaq, L. Li, *Macromolecules* **2022**, *55*, 1398.
[24] T. Yamamoto, Y. Tezuka, *Soft Matter* **2015**, *11*, 7458.
[25] S.-Z. He, M. Holger, C.-F. Su, C.-X. Wu, *Chin. Phys. B* **2013**, *22*, 016101.
[26] W. Qiu, B. Li, Q. Wang, *Soft Matter* **2018**, *14*, 1887.
[27] W.-B. Wan, H.-H. Lv, H. Merlitz, C.-X. Wu, *Chin. Phys. B* **2016**, *25*, 106101.
[28] M. Romio, L. Trachsel, G. Morgese, S. N. Ramakrishna, N. D. Spencer, E. M. Benetti, *ACS Macro Lett.* **2020**, *9*, 1024.
[29] M. Jehser, G. Zifferer, C. Likos, *Polymers (Basel)* **2019**, *11*, 541.
[30] S. A. Egorov, *Macromol. Theory Simul.* **2022**, *31*, 2100065.
[31] G. Morgese, B. Shirmardi Shaghasemi, V. Causin, M. Zenobi-Wong, S. N. Ramakrishna, E. Reimhult, E. M. Benetti, *Angew. Chem., Int. Ed.* **2017**, *56*, 4507.
[32] S. N. Ramakrishna, G. Morgese, M. Zenobi-Wong, E. M. Benetti, *Macromolecules* **2019**, *52*, 1632.
[33] U. Raviv, S. Giasson, N. Kampf, J.-F. Gohy, R. Jérôme, J. Klein, *Nature* **2003**, *425*, 163.
[34] W. H. Briscoe, S. Titmuss, F. Tiberg, R. K. Thomas, D. J. Mcgillivray, J. Klein, *Nature* **2006**, *444*, 191.
[35] R. C. Advincula, W. J. Brittain, K. C. Caster, J. Ruhe, *Polymer Brushes: Synthesis, Characterization, Applications*, Wiley-VCH, Weinheim **2005**.
[36] A. Halperin, *Langmuir* **1999**, *15*, 2525.
[37] A. Hucknall, S. Rangarajan, A. Chilkoti, *Adv. Mater.* **2009**, *21*, 2441.
[38] H. C. Mccaig, E. Myers, N. S. Lewis, M. L. Roukes, *Nano Lett.* **2014**, *14*, 3728.
[39] T. Wang, Y. Yu, D. Chen, S. Wang, X. Zhang, Y. Li, J. Zhang, Y. Fu, *Nanoscale* **2017**, *9*, 1925.
[40] G. C. Ritsema Van Eck, L. Chiappisi, S. De Beer, *ACS Appl. Polym. Mater.* **2022**, *4*, 3062.
[41] H. Yang, H. Zhu, M. M. R. M. Hendrix, N. J. H. G. M. Lousberg, G. De With, A. C. C. Esteves, J. H. Xin, *Adv. Mater.* **2013**, *25*, 1150.
[42] Q.i Zhong, E. Metwalli, M. Rawolle, G. Kaune, A. M. Bivigou-Koumba, A. Laschewsky, C. M. Papadakis, R. Cubitt, P. Müller-Buschbaum, *Macromolecules* **2015**, *48*, 3604.
[43] Q.i Zhong, E. Metwalli, M. Rawolle, G. Kaune, A. M. Bivigou-Koumba, A. Laschewsky, C. M. Papadakis, R. Cubitt, J. Wang, P. Müller-Buschbaum, *Macromolecules* **2016**, *49*, 317.
[44] T. Saerbeck, R. Cubitt, A. Wildes, G. Manzin, K. H. Andersen, P. Gutfreund, *J. Appl. Crystallogr.* **2018**, *51*, 249.
[45] G. Morgese, B. Verbraeken, S. N. Ramakrishna, Y. Gombert, E. Cavalli, J.-G. Rosenboom, M. Zenobi-Wong, N. D. Spencer, R. Hoogenboom, E. M. Benetti, *Angew. Chem., Int. Ed.* **2018**, *57*, 11667.
[46] W. Hassouneh, E. B. Zhulina, A. Chilkoti, M. Rubinstein, *Macromolecules* **2015**, *48*, 4183.
[47] N. T. Moore, A. Y. Grosberg, *Phys. Rev. E* **2005**, *72*, 61803.
[48] T. Widmann, L. P. Kreuzer, G. Mangiapia, M. Haese, H. Frielinghaus, P. Müller-Buschbaum, *Rev. Sci. Instrum.* **2020**, *91*, 113903.
[49] C. Geiger, J. Reitenbach, L. P. Kreuzer, T. Widmann, P. Wang, R. Cubitt, C. Henschel, A. Laschewsky, C. M. Papadakis, P. Müller-Buschbaum, *Macromolecules* **2021**, *54*, 3517.
[50] P. Müller-Buschbaum, R. Cubitt, C. Geiger, L. P. Kreuzer, J. Reitenbach, T. Saerbeck, A. Vagias, E. M. Benetti, P. Wang, Q. Zhong, Kinetics of Controlled Transfer of Water Molecules Between Light- and Thermo- Responsive Polymer Layers in Films. Institut Laue-Langevin (ILL). https://doi.org/10.5291/ILL-DATA.9-11-1956.
[51] R. Cubitt, T. Saerbeck, R. A. Campbell, R. Barker, P. Gutfreund, *J. Appl. Crystallogr.* **2015**, *48*, 2006.
[52] A. R. J. Nelson, S. W. Prescott, *J. Appl. Crystallogr.* **2019**, *52*, 193.
[53] G. C. Ritsema Van Eck, L. B. Veldscholte, J. H. W. H. Nijkamp, S. De Beer, *Macromolecules* **2020**, *53*, 8428.
[54] A. Karim, S. K. Satija, J. F. Douglas, J. F. Ankner, L. J. Fetters, *Phys. Rev. Lett.* **1994**, *73*, 3407.
[55] B. D. Vogt, C. L. Soles, R. L. Jones, C.-Y. Wang, E. K. Lin, W.-L. Wu, S. K. Satija, D. L. Goldfarb, M. Angelopoulos, *Langmuir* **2004**, *20*, 5285.
[56] T. Widmann, L. P. Kreuzer, N. Hohn, L. Bießmann, K. Wang, S. Rinner, J.-F. Moulin, A. J. Schmid, Y. Hannappel, O. Wrede, M. Kühnhammer, T. Hellweg, R. Von Klitzing, P. Müller-Buschbaum, *Langmuir* **2019**, *35*, 16341.
[57] L. P. Kreuzer, T. Widmann, C. Geiger, P. Wang, A. Vagias, J. E. Heger, M. Haese, V. Hildebrand, A. Laschewsky, C. M. Papadakis, P. Müller-Buschbaum, *Langmuir* **2021**, *37*, 9179.
[58] O. Löhmann, S. Micciulla, O. Soltwedel, E. Schneck, R. Von Klitzing, *Macromolecules* **2018**, *51*, 2996.
[59] G. Morgese, L. Trachsel, M. Romio, M. Divandari, S. N. Ramakrishna, E. M. Benetti, *Angew. Chem., Int. Ed.* **2016**, *55*, 15583.
[60] E. Eiser, J. Klein, T. A. Witten, L. J. Fetters, *Phys. Rev. Lett.* **1999**, *82*, 5076.
[61] T. Sakaue, *Soft Matter* **2018**, *14*, 7507.
[62] T. Sakaue, *React. Funct. Polym.* **2019**, *134*, 150.
[63] C. J. Galvin, M. D. Dimitriou, S. K. Satija, J. Genzer, *J. Am. Chem. Soc.* **2014**, *136*, 12737.
[64] J. Jaczewska, I. Raptis, A. Budkowski, D. Goustouridis, J. Raczkowska, M. Sanopoulou, E. Pamuła, A. Bernasik, J. Rysz, *Synth. Met.* **2007**, *157*, 726.
[65] T. Sakaue, C. H. Nakajima, *Phys. Rev. E* **2016**, *93*, 42502.
[66] L. J. Fetters, D. J. Lohse, D. Richter, T. A. Witten, A. Zirkel, *Macromolecules* **1994**, *27*, 4639.
[67] M. Doi, S. F. Edwards, *The Theory of Polymer Dynamics*, Clarendon Press, Oxford **1986**.

